

# Galaxy formation and evolution in a cosmological context: news from hydrodynamical simulations

R. Domínguez-Tenreiro<sup>1</sup>, C. A. Brook<sup>1</sup>, J. Casado<sup>1</sup>, M. Doménech<sup>2</sup>, F.J. Martínez-Serrano<sup>2</sup>, M. Mollá<sup>3</sup>, A. Obreja<sup>1</sup>, J. Oñorbe<sup>4</sup>, A. Serna<sup>2</sup>, and G. Stinson<sup>5</sup>

<sup>1</sup> Dpto. de Física Teórica, Univ. Autónoma de Madrid, 28049 Cantoblanco, Madrid, Spain

<sup>2</sup> Dpto. de Física y A. C., Univ. Miguel Hernández, 03202 Elche, Spain

<sup>3</sup> Depto. de Investigación Básica, CIEMAT, 28040 Madrid, Spain

<sup>4</sup> Center for Cosmology, Dept. of Physics and Astronomy, Univ. of California, Irvine, USA

<sup>5</sup> Max-Planck-Institut für Astronomie, Königstuhl 17, 69117 Heidelberg, Germany

## Abstract

We briefly report on some of the physical laws and processes relevant to galaxy formation and evolution in a cosmological context. Some results will be presented relative to spiral galaxies, as well as to galaxy groupings and the dark matter versus galaxy connection. Particular attention will be paid to the question of how well can the galaxy assembly processes as evinced by simulations be explained by the basic physical theories we report on. A positive answer allows us to use the simulations as a tool to understand some of the complex physical processes underlying galaxy formation and evolution that cannot be directly observed.

## 1 Introduction

An outstanding problems in astrophysics and cosmology is how and when galaxies formed within the framework of the expanding universe and in the presence of a huge amount of dark matter relative to their luminous content, making the dark matter versus galaxy connection one of the relevant pieces of this puzzle. This connection is described at the short scales, where the non-linear processes dominate the evolution, by the so-called *Halo Model*, or the statistical relationship among halo mass and its occupation by galaxies. Observations provide with the galaxy distribution, quantified through statistical tools. The dark-matter distribution, however, is not directly available from observations, just some input from clustering and lensing analyses. To interpret them, we need a theoretical model for clustering or hydrodynamical simulations.

Another relevant pieces of the puzzle are the properties of the stellar populations, and

more so, the possibility that these properties are different according to the moment when the stars formed. In fact, a two-phase scenario for dark halos as well as for massive galaxies mass assembly has been reported, these two phases reflecting in fact the local collapse-like contractive deformations of local regions of the expanding universe, as described by the the adhesion model generalization of the popular Zeldovich theory. Here we report on an extension of the two-phase scenario to interpret bulge and disk formation in intermediate mass galaxies. High resolution hydrodynamical simulations are also a convenient tool in this case. The simulations have been run either with the P-DEVA or GASOLINE codes, codes which regulate star formation in very different ways, with the first simulations inputting low star formation efficiency under the assumption that feedback occurs on subgrid scales, while the GASOLINE simulations have feedback which drives large scale outflows.

## 2 Some theoretical developments on galaxy formation

### 2.1 The halo occupation distribution

The modern language to describe analytically the clustering of galaxies and its connection to the underlying mass clustering is the so-called *Halo Occupation Distribution (HOD) model* see [7], for a review; see also [25] and [31]). This is a statistical description based on the conditional stellar mass function,  $\Phi(M_*|M_h)$ , which represents the number of galaxies with stellar mass in the interval  $M_* \pm dM_*/2$  at fixed halo mass  $M_h$ . The conditional stellar mass function can be divided into two contributions, one coming from halo central galaxies, and the other from the halo satellites:  $\Phi(M_*|M_h) = \Phi_c(M_*|M_h) + \Phi_s(M_*|M_h)$ . In the absence of any theoretical or observational guidance, the functional forms for both  $\Phi_c(M_*|M_h)$  and  $\Phi_s(M_*|M_h)$  are to be modelled (see, for example, [16] for a recent formulation). Once they are, the central (satellite) occupation function  $\langle N_{cen}(M_h|char) \rangle$  ( $\langle N_{sat}(M_h|char) \rangle$ ), that is, the average number of central (satellites) galaxies of given characteristics that are hosted by a halo of mass  $M_h$ , can be easily calculated.

The HOD model has a wider range of possibilities to connect the observational galaxy distribution to that of dark matter. However, as said above, its formulation demands several analytical relationships that miss any theoretical or direct observational guidance, and moreover they have a number of free parameters. Even if current HOD formulations lead to nice results on galaxy clustering and other statistics of galaxy distribution, HOD models demand to be studied with other methodologies as well. A common and powerful method is to use hydrodynamical simulations in a cosmological context.

### 2.2 Advanced non-linear stages of gravitational instability

The results of a self-consistent simulation will be more easily understood in the context of physical theories for the advanced non-linear stages of gravitational instability, provided by the Zeldovich approximation [29] and its extension to the adhesion model [12, 23, 26], including singularity dressing [9] and gas physics. The adhesion model has been introduced to avoid multistreaming, by adding a small diffusion term in Zeldovich's momentum equation,

in such a way that it has an effect only when and where mass element crossings are about to take place. It can be shown that, in this case, the solutions for the velocity field behave just as those of Burgers' equation [3] in the limit  $\nu \rightarrow 0$ , whose analytical solutions are known. The most significant characteristic of Burgers' equation solutions is that they unavoidably develop singularities (caustics), i.e., locations where at a given time the velocity field becomes discontinuous and mass elements coalesce, resulting in some regions undergoing collapse-like contractive deformations with different geometries. In this respect, we are led to the theory of the so-called *singular flows*. This approximation has already been used in the context of N-body simulations to predict when and where large scale singularities or caustics (i.e., the skeleton of the large scale mass distribution) form [28]

We note that the adhesion model has no predictions about the inner caustic structure. However it has been shown that velocity dispersion halts collapse, giving rise to singularity dressing [9]. Therefore, here we will use the adhesion model as a theoretical framework to guide our understanding on the mass assembly of galaxies as an accretion process onto caustics or "caustic dressing" at smaller scales, including the implications that different aspects of the dynamics of singular flows in an expanding universe could have on the mass assembly processes of galaxies. Hydrodynamical simulations in a cosmological context are necessary to understand how gas and star formation behave in this scenario [11].

### 2.3 Two-phase halo mass assembly

Analytical models [21], as well as N-body simulations [27, 30], have shown that two different phases can be distinguished along *halo* mass assembly: i) first, a violent, fast phase, with high mass aggregation (i.e., merger) rates, ii) later on, a slow phase, where the mass aggregation rates are much lower. Hydrodynamical simulations have confirmed this scenario and its implications for properties of massive galactic objects at low  $z$ , see [10, 11, 19, 6], as well as in bulge formation [18]. These two phases in a sense follow from the unavoidability of local collapse, as explained above, and in this paper, we present results involving disk formation as well.

## 3 Introducing simulations

We use P-DEVA, the OpenMP parallel version of the DEVA code [22], which includes the chemical feedback and cooling methods described in [17], and in which the conservation laws (e.g. momentum, energy, angular momentum and entropy) hold accurately. To work on the dark-matter versus galaxy connection problem, large dynamical range hydrodynamical simulations are required. We present here results from the GALFOBS simulation, with a dynamical range of  $5 \times 10^4$ , and a periodic volume of  $80 \text{ Mpc}^3$ , large enough to properly account for large-scale clustering effects [20]. On the other side, high-resolution simulations are required to study bulge and disk formation in a cosmological context. To this end, we analyzed a set of runs first presented in [8]. The star formation recipe follows a Kennicutt – Schmidt-like law, where, in line with [1], we implement inefficient SF parameters which implicitly account for feedback by mimicking its effects, assumed to work on sub-grid scales.

The `GASOLINE` code has also been used. In this code, the effective star formation rates are determined by the combination and interplay of star efficiency and feedback. Supernova feedback is implemented using the blastwave formalism [24]. To mimic the weak coupling of this energy to the surrounding gas, pure thermal energy feedback was injected, which is highly inefficient in these types of simulations [13, 14], making an effective coupling of the order of 1%.

## 4 HOD estimation from large hydrodynamical simulations

Cosmological hydrodynamical simulations with high dynamical range offer us invaluable opportunities to deepen our understanding of this problem. Such simulations are hard to run, and in fact very few results were available until now. We present here first results of the Halo Occupation Distribution measurements on the GALFOBS simulation. The measurements have been made at different redshifts and on different mass-limited simulated galaxy samples, using as galaxy finder the JUMP Detector (JUMP-D) [15], see also [5]. JUMP-D aims at finding and measuring central and satellite galaxies within given host haloes, i.e. *baryonic* substructure objects within a sphere of given radius  $R_{\text{lim}}$  about the centre of the host. To this extent the stellar and gas mass profiles are searched for jumps (and hence the name) in the three-dimensional accumulated mass profiles from the host halo centre out to the limiting radius  $R_{\text{lim}}$  (i.e. usually the host halo’s virial radius). The jump detection criterion is based on the detection of changes in the first and second derivatives of the respective mass profiles in the  $r, \theta$  and  $\phi$  variables at the substructure locations corresponding to the jumps they cause. These results from the mass profile are used as a first satellite detection (i.e., location and velocity), that is later on refined by searching for maxima in 6-dimensional phase-space within an allowance region about that first center.

Figure 1 summarizes our up-to-date most relevant results. There we can see that the average number of satellites hosted by halos of given mass are consistent with observations for massive satellites (left). We also see (right) that halo DM mass density profiles are consistently traced by their satellite number distributions, at least for massive enough halos.

## 5 Bulge and disk formation

We first present here the results of an analysis and comparison of the bulges of a sample of  $L_*$  spiral galaxies formed in hydrodynamical simulations in a cosmological context, using two different codes, P-DEVA and `GASOLINE`. Figure 2 show synthetic images of the P-DEVA galaxies whose bulges have been analyzed, published in [8].

In all the cases analyzed, the mass aggregation tracks (MATS, they give the evolution of mass inside fixed radii) show a marked knee-like shape, corresponding to the transition from a first fast phase of mass assembly to a later slower one (i.e.,  $t_{\text{cut}}$ ), naturally separating the properties of two populations within the simulated bulges. Figure 3 shows these knees, and their relationship with the important early starburst the galaxies experience, resulting from the collapse-like event closing the fast phase of mass assembly. We can also see that it

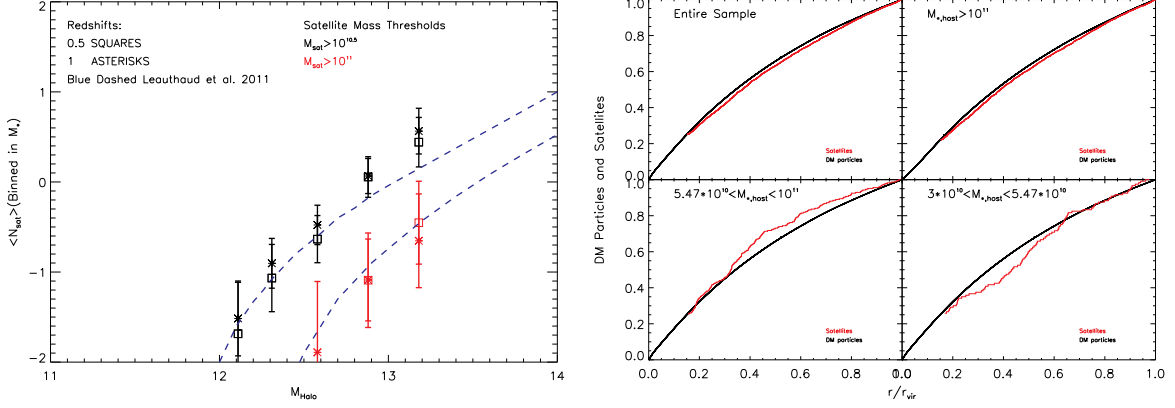


Figure 1: *Left panel:*  $\langle N_{sat}(M_h|char) \rangle$ , the average number of satellite galaxies that are hosted by a halo of mass  $M_h$ . Red and black symbols stand for satellites with stellar masses higher than  $10^{11}$  and  $10^{10} M_{\odot}$ , respectively, while asterisks and squares give results at  $z = 1$  and  $z = 0.5$ . The dashed lines correspond to observation-based results obtained through the analytical HOD model, see [16]. *Right panel:* stacked accumulated number density profiles for the DM particles (black) and satellites (red) populating the halos identified in the GALFOBS simulation at  $z = 0.05$ . Different panels give results corresponding to different ranges in host stellar mass. Both halo and satellite profiles have been normalized.

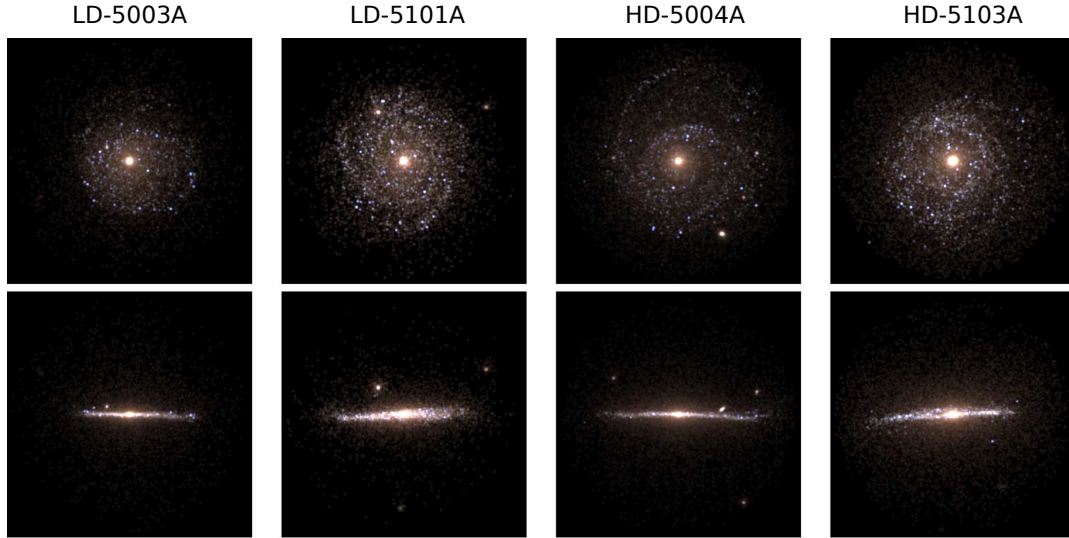


Figure 2: Face-on and edge-on synthetic images obtained using [4] models at  $z = 0$ . All images are 40 kpc side (copyright MNRAS; [8]).

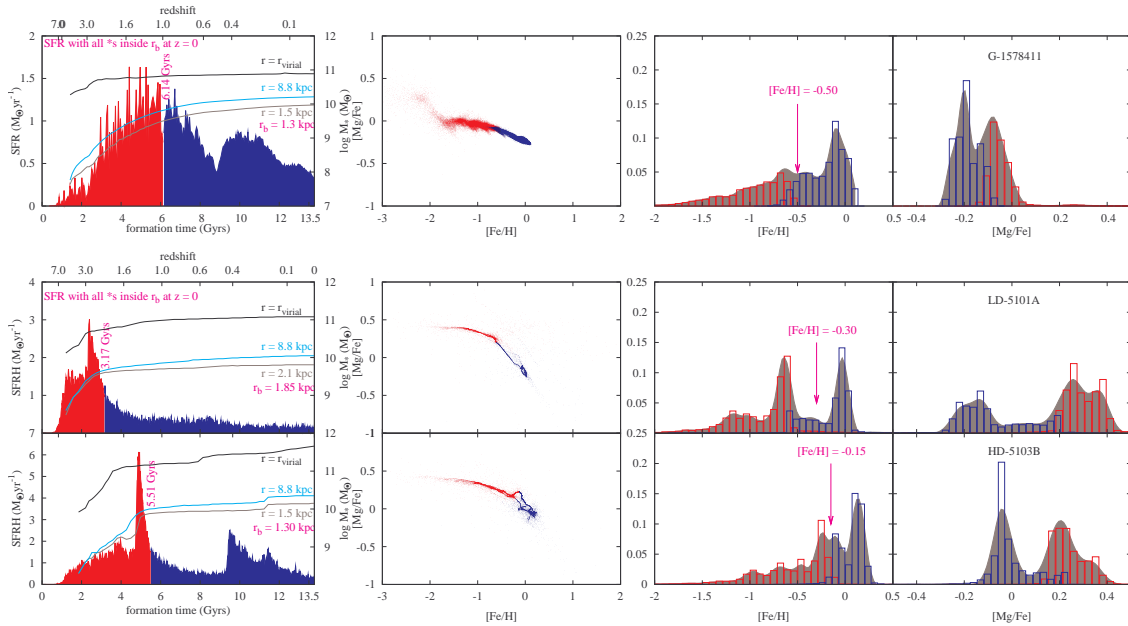


Figure 3: Left column panels give the galaxy MATs (right axis) and SF rates (left axis) of galaxies run with **GASOLINE** (first row) and with **P-DEVA** codes. Black, cyan and grey lines plot the MATs corresponding to radii written with the same colors (virial, disk and bulge scales). The SFRs are in the red (old population) and blue (young population), and include only the formation history of the bulge stellar population at  $z = 0$ . The  $t_{cut}$  values are drawn vertically. Second column panels plot  $[Mg/Fe]$  versus  $[Fe/H]$  for the same galaxies and with the same color code. Their  $[Fe/H]$  and  $[Mg/Fe]$  distributions are shown in columns three and four, respectively.

is followed by a second phase with lower star formation rates, driven by a variety of processes such as disk instabilities and/or mergers (i.e., MAT discontinuities). Classifying bulge stellar particles identified at  $z = 0$  into old and young according to their formation time along any of these phases, we found bulge stellar sub-populations with different kinematics, shapes, stellar ages and metal contents. The old components are less rotationally supported, closer to spherical, with lower metallicity and more alpha-element enhanced than the young ones. Figure 3 clearly illustrates the distinctions regarding the  $[Fe/H]$  and  $[Mg/Fe]$  distributions (an arrow separates the two regimes), as well as their mutual relations.

These results are consistent with the current observational status of bulges, and provide an explanation for some apparently paradoxical observations, such as metal-content gradients and young stellar populations inside bulges. It is remarkable that the trends we have found are robust against the different codes used. Therefore, they must result from basic dynamic properties of flows in an expanding universe, as those described in Section 2.

To study the mass assembly of the whole galaxies (i.e., including disks), we have carried out a detailed follow-up backwards in time of their constituent stellar mass elements, sampled by particles, identified at  $z = 0$ . After that, the configurations they depict at progressively

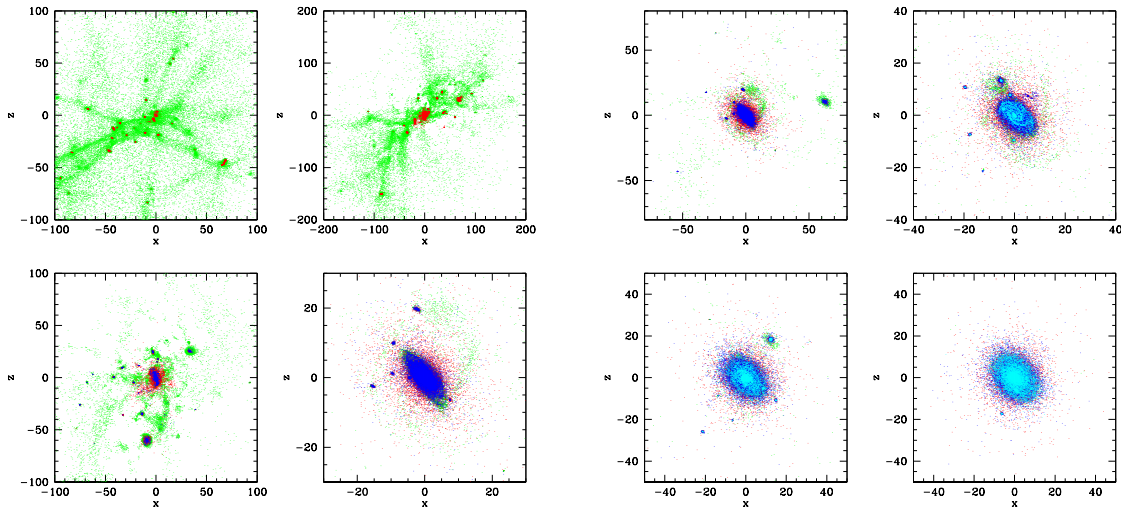


Figure 4: Projections onto the same plane of the positions at different redshifts of those particles that at  $z = 0$  form the stars of the disk galaxy HD5004A (see Fig. 2). Green particles are cold ( $T < 1.0 \times 10^6$ ) gaseous particles at the  $z$  considered; red, blue and cyan are stars formed before, within, and after the universe age range  $0.3 \geq t/t_U \leq 0.6$ . The window sizes are in kpc.

higher  $z$ s were carefully analyzed, showing that the mass assembly histories share common generic patterns irrespective of the code used to run the simulations. Fig. 4 illustrates these common patterns for a P-DEVA galaxy. The 4 panels at the left correspond (from left to right and from top to bottom) to snapshots at  $z = 3.5, 1.75, 1.20$  and  $0.60$ , the first three within the fast phase of mass assembly. The sites where gas is transformed into stars at these early times are clearly visible, as well as the contractive deformations of the early web-like structure to a disk by  $z = 0.60$ . The 4 panels on the right are snapshots at  $z = 0.60, 0.44, 0.30$  and  $0.09$ . Here we see the disk evolution along the slow phase, including small merger events and disk stellar migrations from inside-out. Similar features for GASOLINE galaxies are seen in [2]. These similarities suggest again that basic dynamic properties of flows in an expanding universe (see Section 2) must play a fundamental role as the underlying physical processes in galaxy mass assembly.

## Acknowledgments

This work was partially supported by the MICINN (Spain) through the grants AYA2009-12792-C03-02 and AYA2009-12792-C03-03 from the PNAyA and the "Supercomputaci3n y e-Ciencia" Consolider-Ingenio CSD2007-0050 project. We thank the computer resources provided by BSC/RES (Spain).

## References

- [1] Agertz, O., Teyssier, R., & Moore, B. 2011, MNRAS, 410, 1391

- [2] Brook, C., Stinson, G., Gibson, B.K., Kawata, D., House, E.L., et al. 2012, MNRAS, 426, 690
- [3] Burgers, J.M., 1974, *The Nonlinear Diffusion Equation: Asymptotic Solutions and Statistical Problem*, Reidel, Dordrecht
- [4] Bruzual, G. & Charlot, S. 2003, MNRAS, 344, 1000
- [5] Casado, J., et al. 2013, in preparation
- [6] Cook, M., Lapi, A., & Granato, G. L. 2009, MNRAS, 397, 534
- [7] Cooray, A. & Sheth, R. 2002, Phys. Reports, 372, 1
- [8] Doménech-Moral, M., Martínez-Serrano, F.J., Domínguez-Tenreiro, R., & Serna, A. 2012, MNRAS, 421, 251
- [9] Domínguez, A. 2000, Phys. Rev. D, 62, 103501
- [10] Domínguez-Tenreiro, R., Oñorbe, J., Sáiz, A., Artal, H., & Serna, A. 2006, ApJ, 636L, 77
- [11] Domínguez-Tenreiro, R., Oñorbe, J., Martínez-Serrano, F.J., & Serna, A. 2011, MNRAS, 413, 302
- [12] Gurbatov, S. N., Saichev, A. I., & Shandarin, S. F. 1989, MNRAS, 236, 385
- [13] Katz, N. 1992, ApJ, 391, 502
- [14] Kay, S. T., Pearce, F. R., Frenk, C. S., & Jenkins, A. 2002, MNRAS, 330, 113
- [15] Knebe, A., Libeskind, N.I., Pearce, F., Behroozi, P., & Casado, J., et al. 2012, MNRAS in press
- [16] Leauthaud, A., Tinker, J., Behroozi, P. S., Busha, M. T., & Wechsler, R. H. 2011, ApJ, 738, 45
- [17] Martínez-Serrano, F. J., Serna, A., Domínguez-Tenreiro, R., & Mollá, M. 2008, MNRAS, 388, 3
- [18] Obreja, A., Domínguez-Tenreiro R., Brook, C.A. et al. 2012, ApJ, submitted
- [19] Oser, L., Ostriker, J. P., Naab, T., Johansson, P. H., & Burkert, A. 2010, ApJ, 725, 2312
- [20] Power, C. & Knebe, A. 2006, MNRAS, 370, 691
- [21] Salvador-Solé, E., Manrique, A., & Solanes, J.M. 2005, MNRAS, 358, 901
- [22] Serna, A., Domínguez-Tenreiro, R., & Sáiz, A. 2003, ApJ, 597, 878
- [23] Shandarin, S. F. & Zeldovich, Y. B. 1989, *Reviews of Modern Physics*, 61, 185
- [24] Stinson, G., Seth, A., Katz, N., et al. 2006, MNRAS, 373, 1074
- [25] Tinker, J. L., Weinberg, D. H., Zheng, Z., & Zehavi, I. 2005, ApJ, 631, 41
- [26] Vergassola, M., Dubrulle, B., Frisch, U., & Noullez, A. 1994, A&A, 289, 325
- [27] Wechsler, R.H., Bullock, J.S., Primack, J.R., & Kravtsov, A.V., Dekel A., 2002, ApJ, 568, 52
- [28] Weinberg, D. H. & Gunn, J. E. 1990, MNRAS, 247, 260
- [29] Zeldovich Y. B. 1970, A&A, 5, 84
- [30] Zhao, D.H., Mo, H.J., Jing, Y.P., & Borner, G., 2003, MNRAS, 339, 12
- [31] Zheng, X. Z., Hammer, F., Flores, H., Assémat, F., & Rawat, A. 2005, A&A, 435, 507